Int. J. Electrochem. Sci., 13 **(2018)** 11203 – 11214, doi: 10.20964/2018.11.81

International Journal of ELECTROCHEMICAL SCIENCE
www.electrochemsci.org

Short Communication

Preparation of High Contents of Pyridinic and Pyrrolic-Nitrogen Doped Activated-Carbon from Pyrolysis of Purple Cabbage for the Catalysis of Oxygen Reduction Reaction

Jing Cheng[1†], *Yao Liu*[1†], *Yanrong Li*[1†], *Wenli Liao*[1†], *Zhongbin Li*[1], *Chaozhong Guo*[1,*], *Wei−Zhong Zhang*[2], *Rong Hu*[1,*], *Qin−Rong Kang*[2], *Jianglan Liao*[1], *Wensheng Li*[4], *Linzheng Liao*[1,*]

[1] Research Institute for New Materials Technology, School of Materials and Chemical Engineering, Engineering Research Center of New Energy Storage Devices and Applications, Chongqing University of Arts and Sciences, Chongqing 402160, China.
[2] School of Resources and Civil Engineering, Wuhan Institute of Technology, Hubei 430070, China.
[3] College of Chemistry and Chemical Engineering, Chongqing University, Chongqing 400044, China.
[4] College of Materials Science and Engineering, College of Chemistry and Chemical Engineering, Chongqing University of Technology, Chongqing 400054, China.
[†]These authors contributed equally to this work and should be considered as co-first authors.
[*]E−mail: guochaozhong1987@163.com (C. Guo); 35502657@qq.com (R. Hu); 284188178@qq.com (L. Liao)

Received: 15 April 2018 / *Accepted:* 8 June 2018 / *Published:* 1 October 2018

Effective conversion of reproducible organic biomass into valuable carbon material is very important for renewable energy technology. In this study, here we develop a unique strategy to design a nitrogen-doped carbon-based electrocatalyst for oxygen reduction reaction (ORR) *via* successful pyrolysis of purple cabbage combining with $ZnCl_2$ activation and acid-leaching processes. It is found that this carbon material show high ORR catalysis performance with an ORR onset potential of ~0.96 V *versus* RHE and a half-wave potential of ~0.8 V, slightly lower than that of the commercial Pt/C catalyst in 0.1 mol l^{-1} KOH solution. The high ORR activity mainly derives from high contents of pyridinic- and pyrrolic-nitrogen inside the prepared carbon material. Besides, compared to the Pt/C catalyst, the prepared catalyst also exhibits excellent long-term stability, which can be considered as a promising carbon−based ORR catalyst for fuel cells.

Keywords: biomass material, oxygen reduction, porous carbon, electroncatalyst

1. INTRODUCTION

Fuel cells are regarded as a potential alternative to traditional power sources for a wide range of applications owing to their outstanding merits in terms of high efficiency, high energy density and low emissions [1,2]. However, a great disadvantage that the oxygen reduction reaction (ORR) process has a sluggish kinetics behavior at the cathode of fuel cells [3,4]. To date, platinum−based materials are one of the most efficient electrocatalysts for enhancing the ORR catalytic activity. However, high−cost and rarity of metal-Pt limit their practical applications. In addition, poor stability and low tolerance of fuel molecules on the metal-Pt also restrict their applications in fuel cell fields [5−8]. Therefore, the development of highly efficient, low−cost and stable ORR electrocatastlysts is beneficial for the commercialization of fuel cells. Motivated by their economical requirements and excellent performance, the great progress has been achieved in carbon−based Pt-free ORR catalysts. Compared with the 20 wt.% Pt/C catalyst, their exceptional properties such as excellent activity and amazing stability enhance their application [9−14]. Up to now, many types of Pt-free ORR electrocatalysts were reported, including transition metal−nitrogen (M-N_x) compounds [15], complexes of metal oxides and carbon materials [16−19], modified−carbon nanotubes and heteroatoms−doped carbons [20−21]. Thus, high efficiency and long−term stability of these non−Pt catalysts are very important for full cells because of particle growth during long term operation and metal dissolution at high potentials [22−23].

Recently, with the rapid development of transition-metal nitrides (TMNs), they have attracted significant research interests owing to exceptional features, i.e., low−cost, high electronic conductivity and renewability. These materials display a prospective application as Pt−free ORR catalysts. Usually, the TMNs catalysts are synthesized by chemical methods, but the chemical synthesis of TMNs is complicated and low−utilization of metal and the cost of this method are also more expensive than rare metal (Pt, etc.). Hence, more and more researchers focus on green, efficient and convenient natural organic materials towards the ORR by environmentally and economic synthesis methods. For example, several biomass, including pig bone [24], silk fibroin [25], nori [26] and hemoglobin [27] has been widely studied. Obviously, natural organic materials are abundant from amino acids and bioproteins. In our previous work [28,29], several kinds of carbon catalysts with porous nanostructures were prepared *via* the pyrolysis of protein−rich animal blood or soybean biomass. Although the obtained catalysts have exhibited ORR electrocatalyic activity, they do not show the same ORR catalytic activity with the 20 wt.% Pt/C catalyst in alkaline and acid solutions. Therefore, the study of efficient catalysts is still a critical scientific issue for realizing highly−efficient catalysis for oxygen reduction reaction.

Compared to the reported ORR catalysts derived from biomass, purple cabbage (PG) is a lower cost and abundance materials in nature and contains abundant nitrogen content, showing a great potential in producing the ORR catalysis materials. In this study, we develop a facile and new method to prepare a cheap and active ORR electrocatalyst by using PG300 precursor obtained from partial carbonization of PG at 300 °C, combined with zinc chloride ($ZnCl_2$) as an activator. The prepared catalyst was carefully analyzed, and its ORR catalytic activity was evaluated in detail. It suggests that this catalyst has a key function in the electrocatalysis of ORR at alkaline conditions.

2. EXPERIMENTAL

2.1. Materials synthesis

Firstly, fresh PG was purchased from local supermarket and completely dried in vacuum oven at 100 °C for 24 hours. The dried PG was further ground for powders in an agate mortar. Subsequently, 1.0 g of dried PG powder was partially carbonized in a tube furnace at 300 °C for 2 h in nitrogen atmosphere to prepare the precursor (marked PG300). To prepare the PG300Z−X (X=700, 800 or 900) catalyst, the all−solid−state mixture of 0.5 g of zinc chloride (Z) as an activator and 0.1 g of PG300 as a precursor was pyrolyzed at different temperatures (700, 800 and 900 °C) for 2 h with a heating−rate of 5 °C min^{-1} under the flowing−N_2 atmosphere, respectively. The obtained carbon−based catalysts were marked as PG300Z−700, PG300Z−800 and PG300Z−900, respectively. The synthesis process is depicted in Fig. 1. All prepared samples were further washed with 0.5 mol^{-1} HCl solution and dried at 80 °C before using for ORR catalysts.

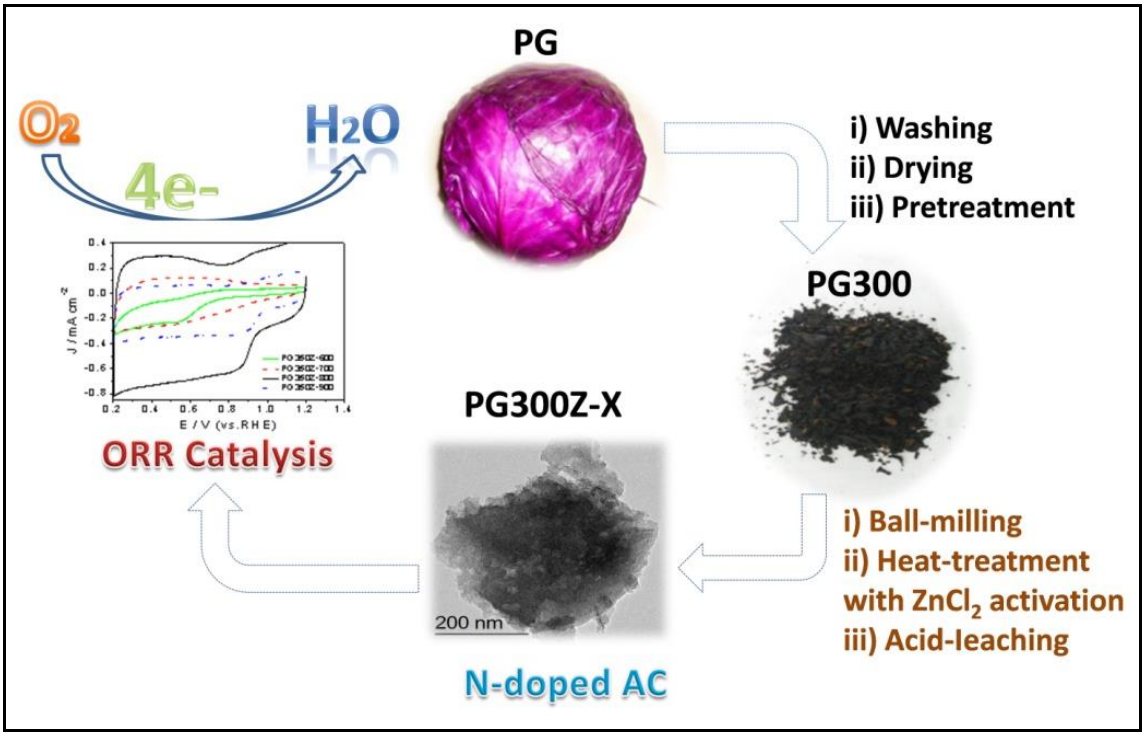

Figure 1. Schematic illustration for synthesis of the PG300Z−X catalyst

2.2. Characterization

The structural analysis of the prepared catalysts was performed *via* using an X−ray photoelectron spectroscopy (XPS) (VG Scientific ESCALAB 220iXL spectrometer) with an Al *K*a (hν = 1486.69 eV) X−ray source. The morphology of the prepared catalysts was characterized by high−resolution transmission electron microscope (FEI Tecnai−G2 F30) with an acceleration voltage of 300 kV.

2.3. ORR performance test

Electrochemical data were obtained on a Zennium−E workstation (Germany) with a conventional three−electrode device. A glass−carbon rotation disk electrode (GC−RDE, Φ=4 mm, Model 636−PAR), a saturated calomel electrode (SCE), and a Pt foil with geometric area of 1 cm^2 were used as a working electrode (WE), a reference electrode (RE), and a auxiliary electrode (AE), respectively. The fabrication of WE refers to our previous reports [28]. The mass loading is controlled to be around 0.40 mg cm^{-2} except for the commercial Pt/C catalyst (20 wt.% Pt) with a mass loading of 0.30 mg cm^{-2}. All potentials *versus* SCE were transformed into the potentials *versus* a reversible hydrogen electrode (RHE). All electrochemical experiments including cyclic voltammetry (CV) and linear sweep voltammetry (LSV) tests were carried out in 0.1 mol L^{-1} KOH electrolytes at a scanning rate of 5 mV s^{-1}. The number of electron transfer (n) per O_2 molecule was calculated by the following equation [26]:

$$\frac{1}{\mathrm{Jd}} = \frac{1}{Jk} + \frac{1}{0.26nFCoDo^{2/3}V^{-1/6}W^{1/2}}$$

where J_d and J_k are the measured current density and kinetic limiting current density respectively, F is the Faraday constant (96,485 C/mol), C_O is the O_2 saturation concentration in the aqueous solution solution (1.2×10^{-6} mol/cm^{-3}), D_O is the O_2 diffusion coefficient in the aqueous solution (cm^2 s^{-1}), v is the kinetic viscosity of the solution (cm^2 s^{-1}), *w* is the electrode rotation rate (r min^{-1}), and 0.26 is a constant when the rotation rate is expressed in rpm.

3. RESULTS AND DISCUSSION

3.1. Morphology and structure characterizations

X−ray photoelection spectroscopy (XPS) was used to probe the electronic structure of PG300Z−700, PG300Z−800 and PG300Z−900. As shown in **Fig. 2**, three typical peaks: C1s, N1s, and O1s can be distinctly found, indicating that all the catalysts consist of carbon, nitrogen and oxygen elements. The total nitrogen contents of PG300Z−700 and PG300Z−800 are about 3.96 at.% and 3.33 at.%, respectively, but that of PG300Z−900 is only 1.70 at.%. It indicates that the increasing of heat−treatment temperature can affect the nitrogen content of the carbon−based catalyst. For the N1s XPS spectra (Fig. 3a−c), the peaks at 398.3, 400.3 and 401.8 eV are attributed to three types of nitrogen functionalities, that is, pyridinic−N, pyrrolic−N and oxidized−N. Generally, the content and proportion of N species in the carbon materials play a vital role for improving the ORR catalytic activity [30,31]. As displayed in Fig. 3d, it is obviously found that the synthesis temperature has an important effect on the relative percentage of various N bonding configurations. In detailed, the relative percentage of the planar N (pyridinic−N and pyrrolic−N) rapidly increases from 73.5 at.% for PG300Z−700 to 79.5 at.% for PG300Z−900 with the increasing carbonization temperatures. Conversely, the percentage of the oxidized−N obviously decreases from 26.5 at.% for PG300Z−700 to 20.5 at.% for PG300Z−900, respectively. The electrocatalytic activity of the catalyst is clearly improved (see Fig. 5). A preliminary conclusion that and the planar−N species can be responsible for the enhancement of the ORR electrocatalytic activity, which may be the electrocatalytically active sites for the ORR [32−33]. Moreover, the structure of PG300Z−800 catalyst (Fig. 4) combined with $ZnCl_2$

activation and heat−treatment at high temperature shows a micro−scaled bulk porous morphology. This micro−structure may facilitate the electron transfer and increase the active sites for the ORR, resulting in good ORR catalytic activity.

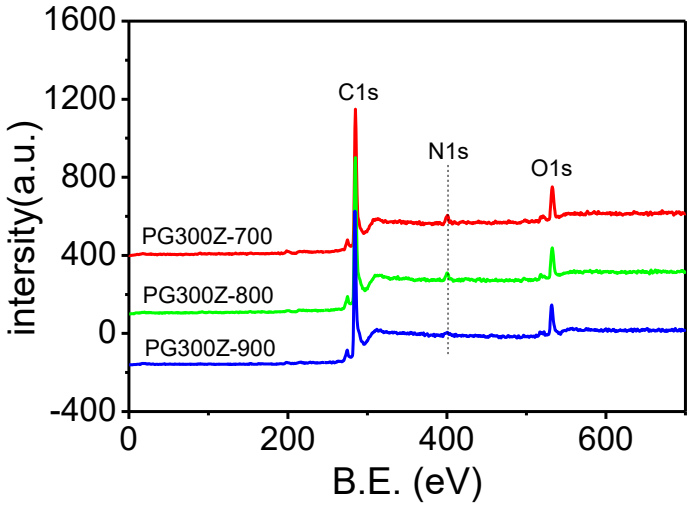

Figure 2. XPS full-scan spectra of PG300Z−700, PG300Z−800 and PG300Z−900.

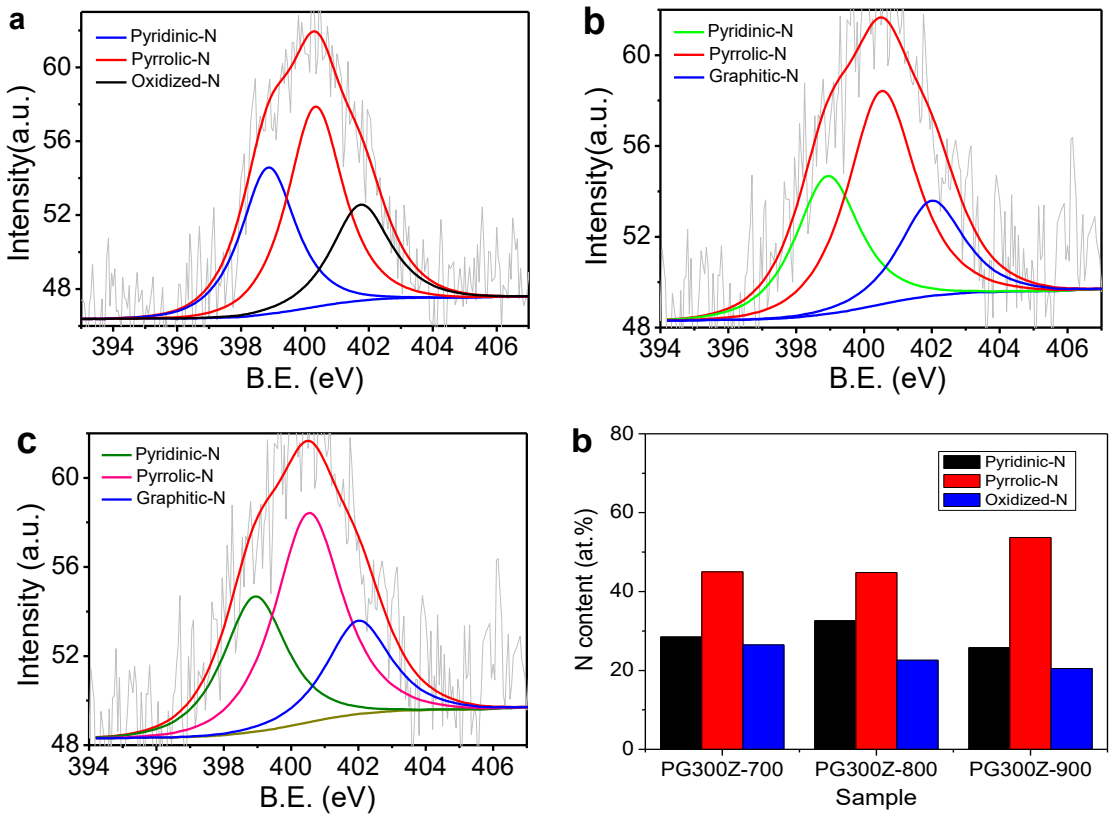

Figure 3. N1s XPS spectra of PG300Z−700 (a), PG300Z−800 (b) and PG300Z−900 (c). (d) The nitrogen group distribution of PG300Z−700, PG300 Z−800 and PG300Z−900.

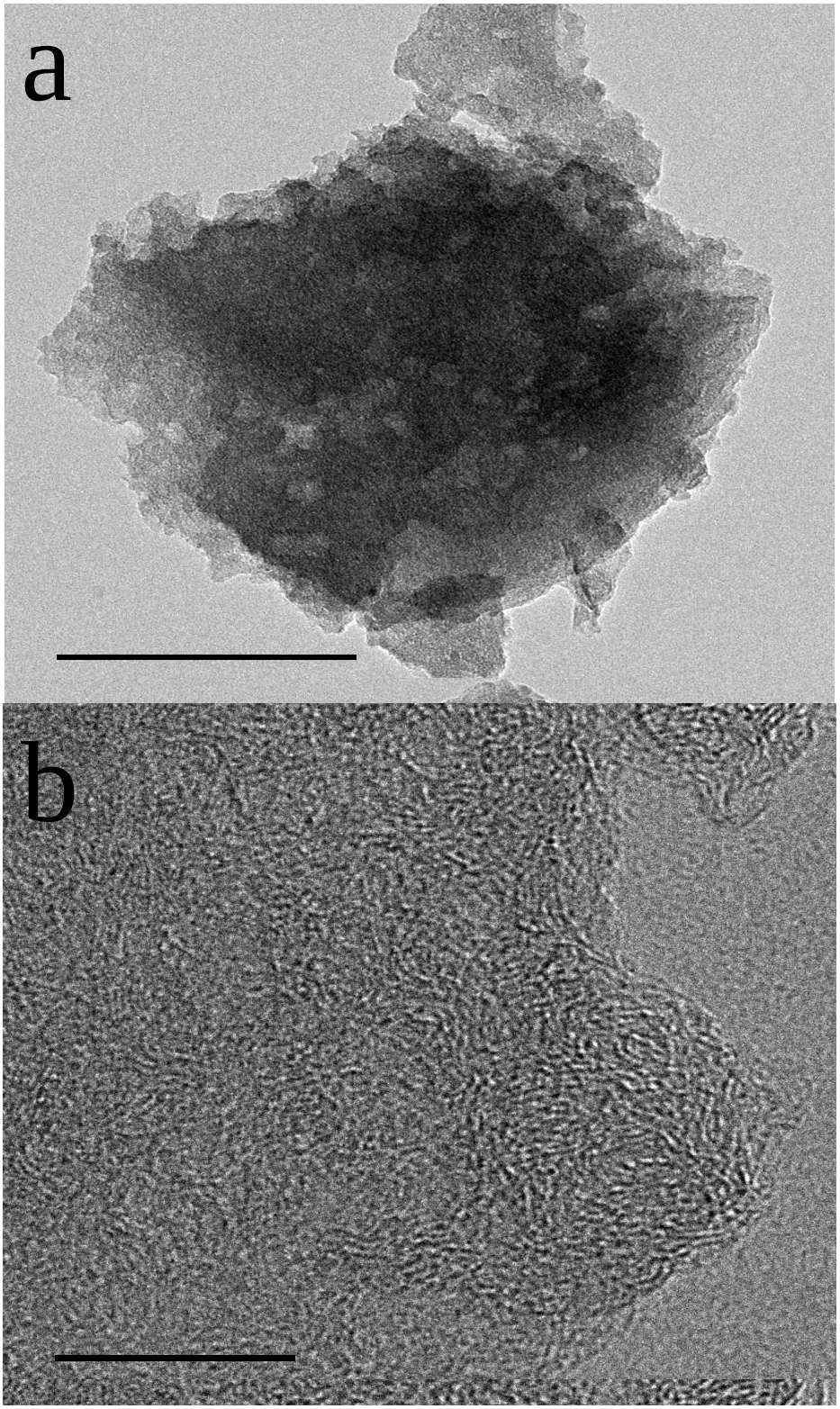

Figure 4. High−resolution TEM images of PG300Z−800 (a, b).

3.2. ORR electrocatalytic activity

In Fig. 5, the electrocatalytic activity towards the ORR of PG300Z−X and 20 wt.% Pt/C catalysts in N_2 *versus* O_2−saturated 0.1 mol l^{-1} KOH solution were evaluated by CV and LSV

methods. As indicated in Fig.3a and 3b, significant differences among the catalysts on ORR catalytic activity in terms of ORR peak potential (E_p) and onset potential (E_{ORR}) are clearly observed by comparing the CV curves obtained in N_2− versus O_2−saturated KOH solutions. Interestingly, the ORR onset potential of PG300Z−800 is up to 0.98V versus RHE, whereas it is only 0.92 V and 0.9 V for PG300Z−900 and PG300Z−700, correspondingly. The varied potential tendency indicates that more contents of pyridinic−N and pyrrolic−N in catalysts have better ORR activity among all the catalysts in alkaline solution. Fig. 5a shows that the CV curve has exhibited no ORR activity in N_2-saturated 0.1 mol l^{-1} KOH solution. The stability of oxygen reduction catalysis is another key factor to evaluate the practical ability of prepared non−precious catalysts in future application of fuel cells. In Fig. 6, we measure the ORR stability of PG300Z−800 and Pt/C catalysts by an accelerated aging test (AAT) with a continuous cyclic voltammetry test for 2000 cycles in O_2−saturated KOH solution at a scan rate of 100 mV s^{-1}. Compared with commercial 20 wt.% Pt/C catalyst, the PG300Z−800 catalyst has better ORR stability. According to the results reported in the literature [24,34−41], it is found that the ORR catalysis performance of PG300Z-800 can compare favourably with some carbon-based electrocatalysts in terms of onset potential, half-wave potential, electron transfer number and current density, as shown in Table 1.

Table 1. The ORR activity data for PG300Z-800 and other carbon catalysts reported in the literature.

Samples	E_{ORR}	$E_{1/2}$	**n**	**Current density**	**Ref.**
Fe/C-SOYB-A	0.83 V *vs*.RHE	0.66 V *vs*.RHE	3.1	1.3 mA cm^{-2} @ + 0.65 V *vs*.RHE	[28]
BP350C1000	0.90 V *vs*.RHE	0.78 V *vs*.RHE	3.5	1.0 mA cm^{-2} @ + 0.65 V *vs*.RHE	[29]
N-Graphene	0.31 V *vs*.SHE	0.35 V *vs*.SHE	3.6	3.0 mA cm^{-2} @ –1.0 V *vs*.SHE	[32]
Co-NC(900)	0.85 V *vs*.RHE	0.80 V *vs*.RHE	3.9	5.5 mA cm^{-2} @ + 0.65 V *vs*.RHE	[34]
CoN/C-600	0.91 V *vs*.RHE	0.85 V *vs*.RHE	3.8	5.7 mA cm^{-2} @ + 0.55 V *vs*.RHE	[35]
N-CNT(800)	0.91 V *vs*.RHE	0.70 V *vs*.RHE	3.7	2.6 mA cm^{-2} @ +0.65 V *vs*.RHE	[36]
GO flakes	–0.21 V *vs*.Ag/AgCl	---	1.9	3.7 mA cm^{-2} @ –1.0 V *vs*.Ag/AgCl	[37]
Co/N/C-900	0.035 V *vs*.Hg/HgO	---	3.8	4.3 mA cm^{-2} @ –0.4 V *vs*. Hg/HgO	[38]

Fe-PANI@ GD-900	1.05 V *vs*.RHE	0.82 V *vs*.RHE	4.0	4.5 mA cm^{-2} @ 0.5 V *vs*.RHE	[39]
PG300Z-800	0.98 V *vs*.RHE	0.80 V vs.RHE	3.9	3.1 mA cm^{-2} @ + 0.65 V *vs*.RHE	This work

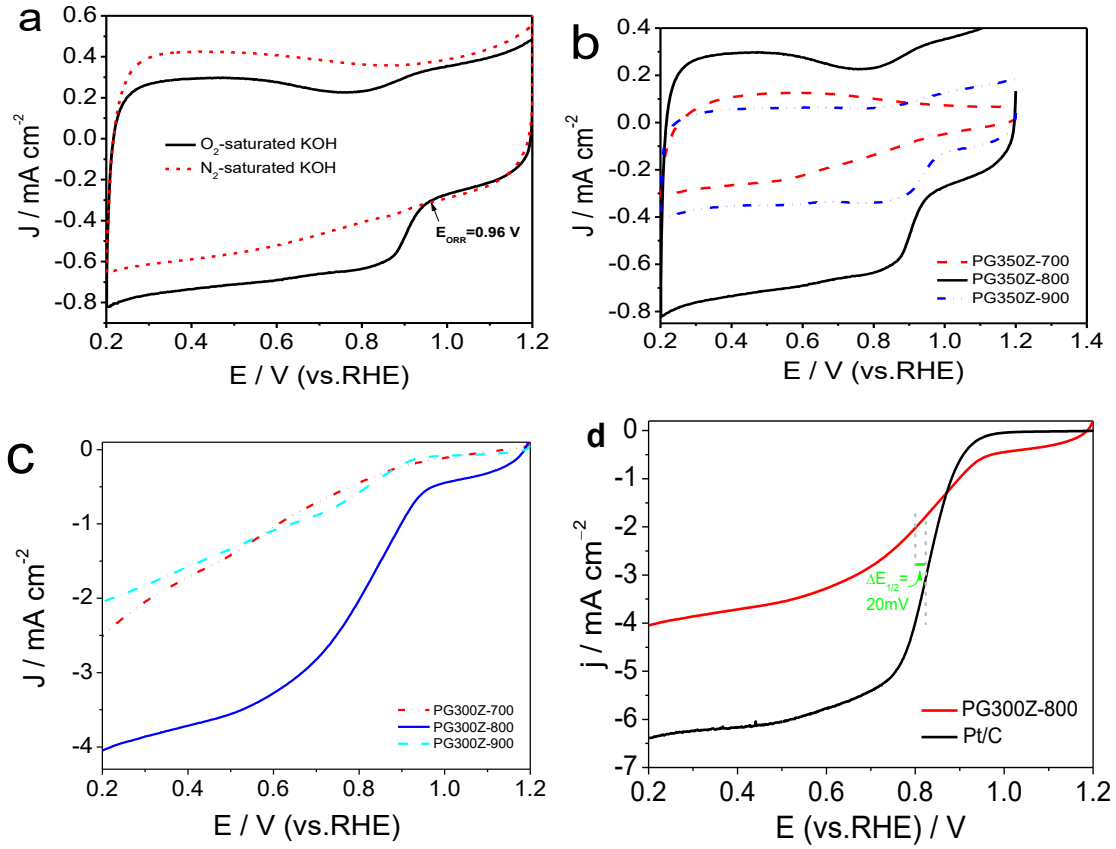

Figure 5. (a) CV curves of PG300Z−800 in O_2 versus N_2−saturated 0.1 mol l^{-1} KOH electrolyte at a scan rate of 5 mV s^{-1}; (b) CV and (c) LSV curves of PG300Z−700, PG300Z−800 and PG300Z−900 in O_2−saturated 0.1 mol l^{-1} KOH electrolyte at a scan rate of 5 mV s^{-1}; (d) LSV curves of PG300Z−800 and 20 wt.% Pt/C catalysts in O_2−saturated 0.1 mol l^{-1} KOH electrolyte.

To further understand the ORR mechanism of PG300Z−800 in KOH solution, the LSV curves for the ORR at different rotation rates from 400 to 3600 rpm were tested and the results were shown in Fig. 7a. It is clearly indicated that the limited current density (j_d) increases with the increasing of the rotation speed. Six j_d values corresponding to the potentials of 0.2, 0.3, 0.4, 0.5, 0.6 and 0.7 V on the LSV curves were taken. According to the slopes of Koutecky−Levich plots, the average electron transfer number is calculated to be ~3.9. It demonstrates the ORR process of PG300Z−800 catalyst involves a four−electron transfer pathway, which is very similar to ORR catalyzed on a Pt/C catalyst in

alkaline electrolyte [41]. Despite the nitrogen−containing functionality plays a critical role in ORR electrocatalytic activity, its reaction mechanism remains unclear until now. In this study, a true fact is certain that the heat-treatment temperature can regulate the ratios of nitrogen species as well as the number of active sites, leading to a great change in ORR catalytic activity. As analyzed from the above XPS data, all the prepared doped-carbon catalysts from $ZnCl_2$ activation at high temperature have high graphitization degree. Especially, the PG300Z−800 with excellent ORR catalytic activity is closely correlated to its nitrogen species and inner porous structure. In addition, the PG300Z−800 catalyst has a relatively high content of nitrogen-containing species including pyridinic− and pyrrolic−N functionalities. Interestingly, a great number of pores can be observed on the surface of PG300Z−800, which also leads to fast electron transfer of oxygen reduction and high ORR activity. After the heat−treatment process at high temperatures, we consider that the pyridinic-N species is also dominant for enhancing the ORR activity of nitrogen-doped carbon-based catalyst other than the pyrrolic−N species. As for pyridinic−N, we infer that it is a primary influence factor on the ORR activity for our system.

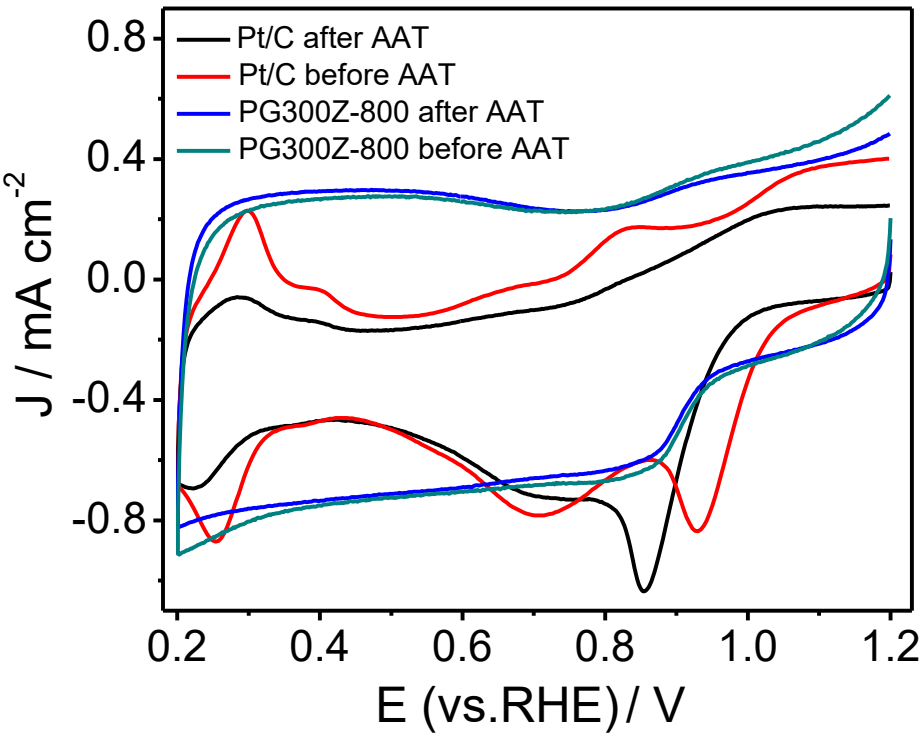

Figure 6. CV curves of PG300Z−800 and 20 wt.% Pt/C catalyst before and after performing an accelerated aging test (AAT) in O_2−saturated 0.1 mol l^{-1} KOH solution.

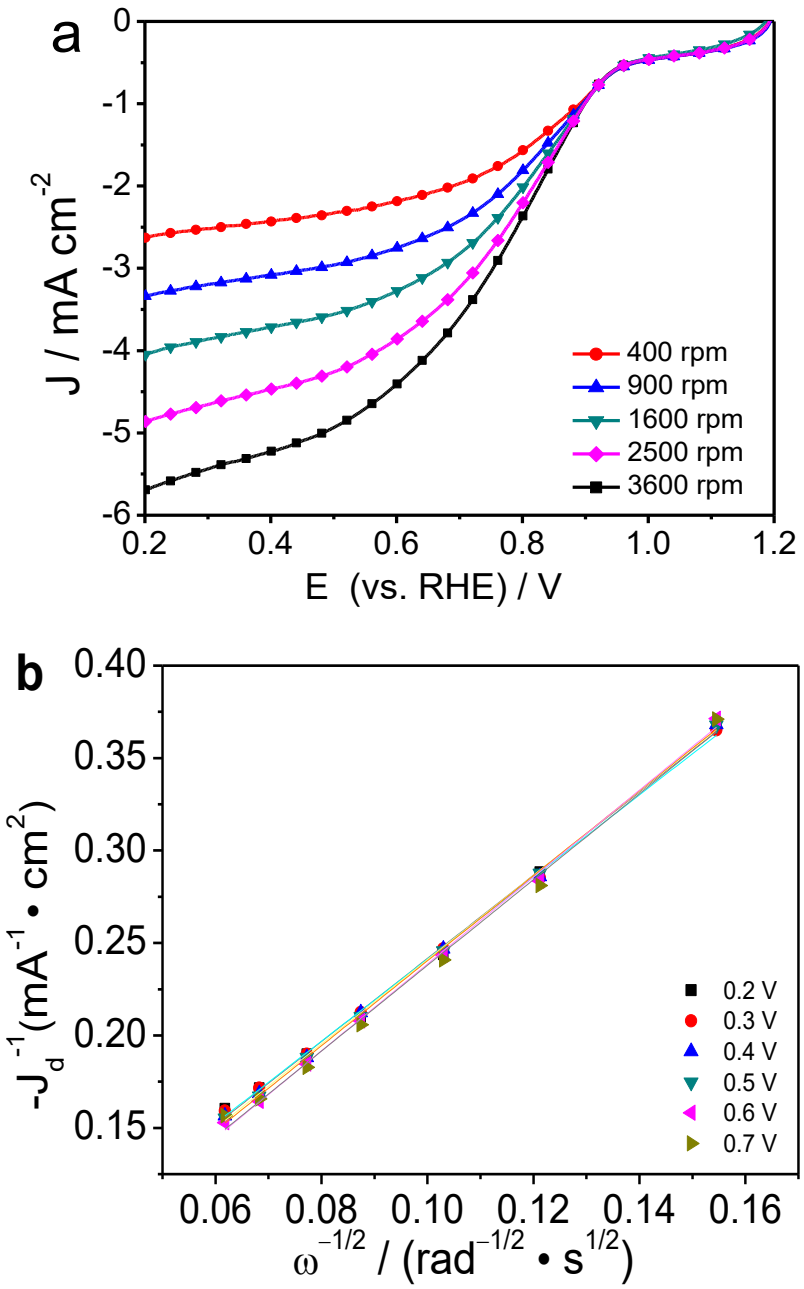

Figure 7. (a) ORR polarization curves of PG300Z−800 obtained at different rotation speeds (400–3600 rpm) in O_2−saturated 0.1 mol l^{-1} KOH electrolyte. (b) Koutecky−Levich plots at different potentials (0.2, 0.3, 0.4, 0.5, 0.6 and 0.7 V). Data are obtained from (a).

4. CONCLUSION

In summary, we develop a novel approach to obtain Pt-free oxygen reduction electrocatalyst by using carbonized purple cabbage as a single-source precursor, combined with $ZnCl_2$ activation and acid-leaching processes. The structure and morphology characterization largely confirm that the surface N−rich active sites of the prepared catalyst are effectively exposed to the oxygen reaction process in alkaline media. Hence, this catalyst exhibits high ORR activity and excellent stability,

which can be comparable to the commercial Pt/C catalyst and other carbon-based catalysts reported in the literature. Furthermore, we propose a new model to explain the relationship between ORR activity and N-rich active structures. Namely, both pyridinic− and pyrrolic−nitrogen species are mainly responsible for the ORR electrocatalytic activity, and they can be further considered as the ORR electrocatalytically active sites for our prepared catalysts. Also, the pyridinic-N species may be a primary influence factor on the ORR activity because of its special importance to the ORR.. Our results demonstrate that the prepared carbon material *via* two-step pyrolysis of purple cabbage biomass with the help of zinc chloride has a promising applications in several electrochemical reactions.

ACKNOWLEDGMENTS
This work was financially supported by the Research Program of Yongchuan Science and Technology Commission (Ycstc2016nc6001), the Scientific and Technological Research Program of Chongqing Municipal Education Commission (KJ1711289, KJ1501118), the Basic and Frontier Research Program of Chongqing Municipality (cstc2015jcyjA50032, cstc2014jcyjA50038), the Scientific Research Program of Chongqing University of Arts and Sciences (P2016XC07, 2017YXC51), the Talent Introduction Project of Chongqing University of Arts and Sciences (R2014CJ02), and the Innovation Team Project of Chongqing Municipal Education Commission (CXTDX201601037). We gratefully thank *Prof.* Changguo Chen, Zhongli Luo, Yujun Si and Jiahong He for helpful discussions.

References

1. M. Zhu, X. Gao, G. Luo and B. Dai, *J. Power Sources*, 225 (2013) 27.
2. N. Larouche, R. Chenitz, M. Lefèvre, E. Proietti and J.−P. Dodelet, *Electrochim. Acta*, 115 (2014) 170.
3. Y. Ma, H. Wang, S. Ji, J. Goh, H. Feng and R. Wang, *Electrochim. Acta*, 133 (2014) 391.
4. Q. Cui, S. Chao, P. Wang, Z. Bai, H. Yan, K. Wang and L. Yang, *RSC Adv.*, 4 (2014) 12168.
5. J. Zhang, S. Wu, X. Chen, K. Cheng, M. Pan and S. Mu, *RSC Adv.*, 4 (2014) 32811.
6. Y. Ye, L. Kuai and B. Geng, *J. Mater. Chem.*, 22 (2012) 19132.
7. V. Goellner, C. Baldizzone, A. Schuppert, M.T. Sougrati, K. Mayrhofer and F. Jaouen, *Phys. Chem. Chem. Phys.*, 16 (2014) 18454.
8. X. Bao, X. Nie, D. von Deak, E.J. Biddinger, W. Luo, A. Asthagiri, U.S. Ozkan and C.M. Hadad, *Top. Catal.*, 56 (2013) 1623.
9. W. Xia, R.Q. Zou, L. An, D.G. Xia and S.J. Guo, *Energy Environ. Sci.*, 8 (2015) 568.
10. L. Hao, S. Zhang, R. Liu, J. Ning, G. Zhang and L. Zhi, *Adv. Mater.*, 27 (2015) 3190.
11. C. You, S. Liao, H. Li, S. Hou, H. Peng, X. Zeng, F. Liu, R. Zheng, Z. Fu and Y. Li, *Carbon*, 69 (2014) 294.
12. C.H. You, S.J. Liao, X.C. Qiao, X.Y. Zeng, F.F. Liu, R.P. Zheng, H.Y. Song, J.H. Zeng and Y.W. Li, *J. Mater. Chem. A*, 2 (2014) 12240.
13. C.H. You, X.Y. Zeng, X.C. Qiao, F.F. Liu, T. Shu, J.H. Zeng, L. Du and S.J. Liao, *Nanoscale*, 7 (2015) 3780.
14. C. You, D. Dang, X. Qiao, G. Wang, W. Fan, R. Chen, Y. Li, X. Li and S. Liao, *J. Mater. Chem. A*, 3 (2015) 23512.
15. H. Yin, C. Zhang, F. Liu and Y. Hou, *Adv. Funct. Mater.*, 24 (2014) 2930.
16. Y. Liang, H. Wang, P. Diao, W. Chang, G. Hong, Y. Li, M. Gong, L. Xie, J. Zhou, J. Wang, T.Z. Regier, F. Wei and H. Dai, *J. Am. Chem. Soc.*, 134 (2012) 15849.
17. J. Xu, P. Gao and T. S. Zhao, *Energy Environ. Sci.*, 5 (2012) 5333.

18. M. Wang, J. Huang, M. Wang, D. Zhang, W. Zhang, W. Li and J. Chen, *Electrochem. Commun.*, 34 (2013) 299.
19. Y. Liang, Y. Li, H. Wang, J. Zhou, J. Wang, T. Regier and H. Dai, *Nature Mater.*, 10 (2011) 780.
20. D. Deng, L. Yu, X. Chen, G. Wang, L. Jin, X. Pan, J. Deng, G. Sun and X. Bao, *Angew. Chem.*, 52 (2013) 371.
21. Y. Li, W. Zhou, H. Wang, L. Xie, Y. Liang, F. Wei, J.C. Idrobo, S.J. Pennycook and H. Dai, *Nature Nanotech.*, 7 (2012) 394.
22. S.J. Hwang, S.K. Kim, J.G. Lee, S.C. Lee, J.H. Jang, P. Kim, T.H. Lim, Y.E. Sung and S.J. Yoo, *J. Am. Chem. Soc.*, 134 (2012) 19508.
23. I.E.L. Stephens, A.S. Bondarenko, U. Gronbjerg, J. Rossmeisl and I. Chorkendorff, *Energy Environ. Sci.*, 5 (2012) 6744.
24. H. Liu, Y. Cao, F. Wang, W. Zhang and Y. Huang, *Electroanal.*, 26 (2014) 1831.
25. F. Liu, H. Peng, C. You, Z. Fu, P. Huang, H. Song and S. Liao, *Electrochim. Acta*, 138 (2014) 353.
26. H. Yang, H. Li, H. Wang, S. Ji, J. Key and R. Wang, *J. Electrochem. Soc.*, 161 (2014) 795.
27. J. Maruyama, J. Okamura and K. Miyazaki, *J. Phys. Chem. C*, 111 (2007) 6597.
28. C. Guo, W. Liao and C. Chen, *J. Power Sources*, 269 (2014) 841.
29. C. Guo, C. Chen and Z. Luo, *J. Power Sources*, 245 (2014) 841.
30. W. Ding, Z. Wei, S. Chen, X. Qi, T. Yang, J. Hu, D. Wang, L. Wan and L. Li, *Angew. Chem.*, 125 (2013) 11971.
31. C. Guo, W. Liao, Z. Li, L. Sun and C. Chen, *Nanoscale*, 7 (2015) 15990.
32. D. Geng, Y. Chen, Y. Chen, Y. Li, R. Li, X. Sun, S. Ye and S. Knight, *Energy Environ. Sci.*, 4 (2011) 760.
33. R. Liu, D. Wu, X. Feng, K. Mullen, *Angew. Chem. Int. Ed.*, 49 (2010) 2565.
34. C. Guo, Y. Wu1, Z. Li, W. Liao, L. Sun, C. Wang, B. Wen, Y. Li and C. Chen, *Nanoscale Res. Lett.*, 12 (2017) 144.
35. S. Chao and M. Jiang , *Int. J. Hydrogen Energ.*, 41 (2016) 12995.
36. J. Zheng, C. Guo, C. Chen, M. Fan, J. Gong, Y. Zhang, T. Zhao, Y. Sun, X. Xu, M. Li, R. Wang, Z. Luo, C. Chen, *Electrochim Acta*, 168 (2015) 386.
37. J. Liu, H. Yang, S. Zhen, C. Poh, A. Chaurasia, J. Luo, X. Wu, E. Yeow, N. Sahoo, J. Lin and Z. Shen, *RSC adv.*, 3 (2013) 11745.
38. H. Wu, C. Guo, J. Li, Z. Ma, Q. Feng and C. Chen, *Int. J. Hydrogen Energ.*, 41 (2016) 20494.
39. Y. Li, C. Guo, J. Li, W. Liao, Z. Li, J. Zhang and C. Chen, *Carbon*, 119 (2017) 201.
40. E. Yeager, *Electrochim. Acta*, 29 (1984)1527.